Published in final edited form as:
Alzheimers Dement. 2013 October ; 9(0): S116–S123. doi:10.1016/j.jalz.2012.10.011.

Focal Hemosiderin Deposits and β-Amyloid Load in the ADNI Cohort

Kejal Kantarci, MD, MS[1], **Jeffrey L. Gunter, PhD**[2], **Nirubol Tosakulwong, BS**[3], **Stephen D. Weigand, MS**[3], **Matthew S. Senjem, MS**[2], **Ronald C. Petersen, MD, PhD**[4], **Paul S Aisen, MD**[5], **William J. Jagust, MD**[6], **Michael W. Weiner, MD**[7], **Clifford R. Jack Jr., MD**[1], and **the Alzheimer's Disease Neuroimaging Initiative**

[1]Department of Radiology, Mayo Clinic, Rochester, MN

[2]Department of Information Technology, Mayo Clinic, Rochester, MN

[3]Department of Biomedical Statistics and Informatics, Mayo Clinic, Rochester, MN

[4]Department of Neurology, Mayo Clinic, Rochester, MN

[5]Department of Neurosciences, University of California – San Diego, La Jolla, CA

[6]Hellen Willis Neuroscience Institute, University of California, Berkeley, CA

[7]Center for Imaging of Neurodegenerative Diseases, VA Medical Center, San Francisco, CA

Abstract

Objective—Prevalence and risk factors for focal hemosiderin deposits are important considerations when planning amyloid–modifying trials for treatment and prevention of Alzheimer's disease (AD).

Methods—Subjects were cognitively normal (n=171), early-mild cognitive impairment (MCI) (n=240), late-MCI (n=111) and AD (n=40) from the Alzheimer's Disease Neuroimaging Initiative (ADNI). Microhemorrhages and superficial siderosis were assessed at baseline and on all available MRIs at 3, 6 and 12 months. β-amyloid load was assessed with ^{18}F-florbetapir PET.

Results—Prevalence of superficial siderosis was 1% and prevalence of microhemorrhages was 25% increasing with age ($p<0.001$) and β-amyloid load ($p<0.001$). Topographic densities of microhemorrhages were highest in the occipital lobes and lowest in the deep/infratentorial regions. A greater number of microhemorrhages at baseline was associated with a greater annualized rate of additional microhemorrhages by last follow-up (rank correlation=0.49;$P<0.001$).

Conclusion—Focal hemosiderin deposits are relatively common in the ADNI cohort and are associated with β-amyloid load.

Keywords

ADNI; microhemorrhage; superficial siderosis; MRI; Amyloid; PET; Florbetapir; Alzheimer's disease; mild cognitive impairment; early mild cognitive impairment

Corresponding Author: Kejal Kantarci, MD, MS, Mayo Clinic 200 First Street SW, Rochester, MN 55905, Phone: 507- 284 8548, Fax: 507–284 2405, kantarci.kejal@mayo.edu.

1. Introduction

Microhemorrhages (mH) and superficial siderosis identified on T2* gradient recalled echo (GRE) and susceptibility weighted MRI are recognized as markers of cerebral microangiopathy in older adults[1, 2]. Risk factors associated with mH include aging[3–5], cerebrovascular disease[6–8], mild cognitive impairment (MCI)[9], Alzheimer's disease (AD)[4, 10], cardiovascular risk factors[3], *APOE* ε4[11, 12] and *APOE* ε2[12] alleles, and higher beta-amyloid (Aβ) load on PET imaging[13].

The prevalence and incidence of mH has recently become an important consideration for inclusion and adverse events in AD therapeutic trials with amyloid-lowering agents[14]. Cerebral amyloid angiopathy (CAA) and associated damage to the media and adventitia of the vasculature is implicated in the pathogenesis of mH in AD[15]. It has been hypothesized that a massive clearance of Aβ with immunotherapy further strains the CAA-impaired vessel wall and increases the risk for mH in AD[16]. Thus, presence of substantial numbers of mH may increase the risk for amyloid-related imaging abnormalities (ARIA) classified as ARIA with mH (ARIA-H) and ARIA with edema (ARIA-E) during amyloid-modifying therapeutic trials. Prevalence and natural history of mH needs to be established to aid in designing amyloid-modifying therapeutic trials, and for interpreting ARIA during these trials for prevention and treatment of AD.

In the current study, we report the prevalence and regional distribution of focal hemosiderin deposits in the form of mH and superficial siderosis in CN, early MCI (EMCI), late MCI (LMCI) and AD subjects in the Alzheimer's Disease Neuroimaging Initiative –Grand Opportunity (ADNI-GO) and ADNI-2 studies. We further investigate the number of mH in relation to *APOE* genotype and Aβ load on PET.

2. Methods

2.1 Subjects

Subjects of this study were ADNI-GO and ADNI-2 participants who underwent 3T MRI studies from June 2010 until March 2012. ADNI is a longitudinal multi-center natural history study designed to characterize clinical, imaging, genetic, and biochemical biomarkers for early detection and tracking of AD[17]. The T2* GRE sequence for the identification of mH and superficial siderosis was added to ADNI MRI protocol in the ADNI-GO study and continued into ADNI-2 with longitudinal studies in the existing ADNI cohort as well as in the new enrollees of the ADNI-GO and ADNI-2 studies[18]. We included all subjects who met the inclusion and exclusion criteria for ADNI-GO and ADNI-2 studies (http://adni-info.org/Scientists/Pdfs/ADNI2_Procedures_Manual_12062011.pdf) and underwent a 3T MRI examination (n=562). Follow-up scans were available in 63 % (n=355) of the study cohort with the last follow-up scans at 3 (n=121), 6 (n=141), and 12 (n=93) months (Supplemental table)

The study cohort was composed of CN (n=171), EMCI (n=240), LMCI (n=111) and AD (n=40) subjects. The diagnostic criteria for CN, EMCI, LMCI and AD in ADNI was previously described [19]. There were 4 subjects (1 CN, 2 LMCI, 1 AD) who were included in ADNI-2 MRI studies but were excluded from this study due to poor quality of the T2* GRE images.

2.2 MRI examination

MRI examinations were performed at 3T scanners at 54 different sites. The MRI sequences used for image analysis in the current study include a 3D MPRAGE and a T2* GRE acquired as described online (http://adni.loni.ucla.edu/research/protocols/mri-protocols/).

2.3 Identification of mH and superficial siderosis

All mH and superficial siderosis were identified by trained image analysts and secondarily confirmed by two radiologists experienced in reading the T2* GRE images (KK and CRJ). Microhemorrhages were defined as homogenous hypointense lesions up to 10 mm in diameter in the gray or white matter on T2* GRE images. All available T2* GRE scans of a subject were used for the rating of individual mH. However, occasionally it was not possible to make a definitive decision, such as distinguishing a mH from a vascular flow-void. In such instances, the mH was labeled as “possible mH”. There were 114 lesions labeled as possible mH (15% of all labeled mH) in the current study. We did not include “possible mH” in the analysis due to the non-definitive nature of the finding. The inter-rater agreement between the two radiologists on definite versus not-definite mH was 85% which corresponded to good agreement (kappa=68%). Superficial siderosis was defined as curvilinear hypointensities overlying the cortical surface, distinct form vascular flow voids.

2.4 Tracking and registration of hemosiderin deposits to a common template

Each mH and or superficial siderosis is tracked independently over all available T2* GRE images. The location of each observed finding is recorded in the coordinate system of the image on which it was made. During evaluation, each T2* GRE image is viewed in its native orientation with no through-plane interpolation to avoid the introduction of artifacts. Other T2* GRE images of the same subject are resampled into the space of the image being evaluated and serve as references. Findings observed on these images are propagated into the coordinate system of the image under evaluation. The mH markings at previous time points are available to the reader when evaluating subsequent T2* GREs. Any mH not marked as possible or definite at previous time points are rated as new mH. A T1 (MPRAGE) image of the subject is registered and resampled into the space of the image under evaluation. The T1 image carries an in-house modified automated anatomic labeling atlas[20] defining bilateral frontal, parietal, temporal and occipital lobar regions, deep/infratentorial gray and white matter regions[21]. Because the lobar regions differ in volume, we compare the regional mH densities as referenced to the volume of the region rather than simply counts per region.

Composite maps of mH locations across subjects are built by transforming T2* GRE image locations into the T1 image space and applying the discrete cosine transformation to template space derived during SPM unified segmentation of the T1 image. A sphere is placed around each microhemhorrage in order to make it visible on 3D rendering; overlapping spheres are allowed to merge forming clusters.

2.5 Amyloid imaging with ^{18}F-florbetapir and image analysis

PET imaging was performed at 54 different sites in 421 (75%) of the subjects. ADNI PET image data was acquired as described online (adni.loni.ucla.edu/about-datasamples/image-data/). Images were averaged, spatially aligned, interpolated to a standard voxel size, and smoothed to a common resolution of 8-mm full width at half maximum.^{18}F-florbetapir PET image volumes of each subject were co-registered to his/her own T1 (MPRAGE) MRI scan with the modified anatomical atlas labels with partial volume correction for tissue and cerebrospinal fluid (CSF) compartments was applied to remove atrophy effects on the ^{18}F-florbetapir uptake on PET images[22]. Whole cerebellar uptake (with partial volume

correction) was used as an internal reference ROI for ^{18}F-florbetapir normalization to calculate ^{18}F-florbetapir standard uptake value ratio (SUVR) images. The global ^{18}F-florbetapir SUVR was calculated by averaging the ^{18}F-florbetapir retention ratio from the bilateral parietal (including posterior cingulate and precuneus), temporal, prefrontal, orbitofrontal, anterior cingulate gray matter regions where the average is weighted by ROI size[23].

2.6 Statistical analysis

The relationship between mH count and age and between mH count and ^{18}F-florbetapir SUVR was tested using Spearman rank-order correlation. Rank correlation was used to test for an association between mH count and clinical group by treating clinical group as an ordinal variable, ordered as CN, EMCI, LMCI and AD. Kruskal-Wallis test was used as a one-way nonparametric ANOVA to evaluate the association between mH count and *APOE* genotype classified as ε2 carriers, ε3/3 homozygotes, and ε4 carriers. The small fraction who were ε2/4 were omitted from this analysis. After grouping all subjects with mH count of 5 or more, we used ordinal logistic regression to evaluate the association between mH count as the response and age, sex, clinical group, *APOE* genotype (three-levels), and log-transformed global ^{18}F-florbetapir. In an exploratory analysis, we used logistic regression to estimate the effect of clinical group or *APOE* genotype on the odds of a mH "event" for three definitions of the event. In model 1 we define the event as the subject having any mHs, in model 2 we define the event as having 2 or more mHs, and in model 3 we define the event as having 3 or more mHs. These models were estimated with and without adjustment for global Aβ load.

3. Results

Characteristics of the study cohort are listed in Table 1. There were age and education level differences across the diagnostic groups. On average, patients with AD were older and patients with EMCI were younger than other diagnostic groups. Proportions of APOE ε4 carriers were greater compared to non-carriers in LMCI and AD versus CN and EMCI ($p=0.002$). The number of mH was associated with age (rank correlation=0.21; $p<0.001$).

While mH were symmetrically distributed in the right and left hemispheres on surface render maps, there were differences in the lobar distribution (Figure 1). Considering the region volumes, mH were concentrated more in the occipital, temporal and parietal lobes compared to the frontal lobes and deep infratentorial region (number/L). The regional mH densities are listed in Table 2. Global ^{18}F-florbetapir SUVR was associated with the number of mH (rank correlation=0.20; $p<0.001$) in the whole brain and when only lobar regions were included in the analysis (rank correlation=0.18; $p<0.001$). Statistically significant relationships between global ^{18}F-florbetapir SUVR and the number of mH was observed only in the frontal and parietal lobar regions. We did not find a topographic relationship between regional ^{18}F-florbetapir SUVR and regional mH densities in the temporal and occipital lobes and the deep/infratentorial region. (Table 2).

Interestingly, the subject with the highest number of mH in the cohort had lower than average global ^{18}F-florbetapir SUVR. This was a 77 year-old EMCI subject with *APOE* genotype of 2/3. The 264 mH at baseline were evenly distributed across the four lobes. The global ^{18}F-florbetapir SUVR was 1.23 and evenly low across the cortex. (Figure 2).

In logistic regression models, *APOE* status was not associated with the presence or absence of mH (model 1). However, *APOE* ε4 carriers had greater odds than *APOE* ε3 homozygotes of having two (model 2; $p=0.046$) and three (model 3; $p=0.03$) or more mH. Although *APOE* ε2 carriers showed trends similar to *APOE* ε4 carriers (i.e. greater odds of having two

and three or more mH compared to *APOE* ε3 homozygotes, this was not statistically significant (P>0.33). We did not find evidence of a statistical interaction between global ^{18}F-AV-45 PET SUVR and *APOE* status in predicting mH as defined by models 1–3. However, we observe that after adjusting for Aβ load, the apparent *APOE* ε4 effect was attenuated while the apparent *APOE* ε2 effect was unchanged (models 1 and 2) or made more prominent (model 3) (Figure 3).

We did not find an association between mH and clinical group (rank correlation=0.06; p=0.17) although prevalence of mH followed a trend from 23% in CN to 25% in EMCI, 28% in LMCI, and 33% in AD. In logistic regression models, the odds of having at least one mH appeared elevated in patient groups relative to CN (model 1). Similarly, the odds of having two or more (model 2) and three or more (model 3) mH tended to be higher in the EMCI, LMCI and AD groups compared to CN. However, the width of the confidence intervals makes this pattern suggestive rather than conclusive.

Superficial siderosis was present in 6 (1%) of the subjects distributed across all clinical groups (1 CN, 2 EMCI, 2 LMCI, and 1 AD) and five of these cases had concurrent mH. *APOE* genotyping was completed in five of the subjects with superficial siderosis and four of them were *APOE* ε4 positive. Median (interquartile range) ^{18}F-florbetapir was not markedly different between patients with superficial siderosis (1.7 (1.5, 1.8)) compared to the rest of the cohort 1.5 (1.4, 1.8) (p=0.16).

There were 90 subjects who had mH at baseline and underwent longitudinal serial MRI with the last scan at 3 (n=30), 6 (n=45), and 12 (n=12) months. With limited follow-up the rank correlation between annual increase in the number of mHs and the baseline mH count was estimated to be 0.49 (p <0.001).

4. Discussion

The major findings of this study were: 1) Superficial siderosis is present in 1% (95% CI, 0.4% to 2%) and one or more definite mH were present in 25% (95% CI, 22% to 29%) of the ADNI cohort, increasing in number with age and Aβ load; 2) The density of mH appear to be highest in the occipital lobes followed by temporal and parietal lobes. Frontal lobes and the deep/infratentorial regions tend to have lower mH densities; 3) APOE ε4 carriers appeared to have greater numbers of mH compared to APOE ε3 homozygotes but this difference was mediated by differences in Aβ load; 4) Greater number of mH at baseline is associated with a faster accumulation of subsequent mH.

Age was a significant predictor of mH independent of the clinical group, consistent with previous reports in older adults with no dementia and AD [3–5]. Furthermore, we found evidence that the number of mH was associated with global Aβ load. The number of mH is associated with ^{11}C-Pittsburgh compound B (PiB) SUVR in CN, MCI and AD subjects[13]. Here we confirm that a similar association exists between the number of mH and global ^{18}F-florbetapir SUVR. This is consistent with the finding that PiB and ^{18}F-florbetapir provide comparable information on Aβ load [24].

The topographic distribution of mH showed greater involvement of the occipital, posterior temporal and parietal regions compared to frontal lobes and deep/infratentorial regions, consistent with previous reports in smaller samples[4, 13]. However, contrary to this distribution of mH, highest ^{18}F-florbetapir SUVR was observed in the parietal and frontal lobe regions with lower levels in the occipital lobes. While there was an association between global ^{18}F-florbetapir SUVR and number of mH in individual subjects, we did not find a relationship between the ^{18}F-florbetapir SUVR and mH densities in the occipital and temporal lobes where the mH densities were highest. Taken together our findings suggest

that ^{18}F-florbetapir SUVR only in-part explain the microangiopathy that underlies mH in older adults. If ^{18}F-florbetapir SUVR is a marker for both vascular and parenchymal Aβ in the brain, ^{18}F-florbetapir should not be expected to specifically localize to areas of vascular Aβ and associated mH[25]. This finding contradicts reports in patients with CAA, in whom greater PiB retention was identified in occipital lobes[26], and focal PiB retention surrounding mH was shown in a case with CAA[27].

Interestingly, the subject with highest number of mH in the ADNI cohort (EMCI subject with 264 mH in Figure 2) had lower than average ^{18}F-florbetapir SUVR. Whereas lobar mH has been associated with CAA, deep/infratentorial mH has been associated with hypertensive or atherosclerotic angiopathy[28]. However it was not possible to attribute the mH in this subject to hypertensive or atherosclerotic angiopathy by regional involvement of the brain with mH because of greater mH densities in lobar regions compared to the deep/infratentorial region. There may be two explanations for the discordance between the number of mH and ^{18}F-florbetapir SUVR in this subject. One explanation is that ^{18}F-florbetapir may have low affinity for vascular amyloid therefore ^{18}F-florbetapir binding may be low in cases with CAA in the absence of significant parenchymal Aβ. While there is no ^{18}F-florbetapir PET data available in pathologically confirmed CAA, the counterargument to this explanation is the co-localization of PiB and mH in CAA[26, 27]. Another explanation is that the kinetics of ^{18}F-florbetapir is different in individuals with significant CAA due to microvascular damage and poor perfusion. Dynamic ^{18}F-florbetapir PET studies and histopathologic evaluations in patients with CAA may further clarify this unexpected finding.

In our sample, *APOE* ε4 carriers had higher numbers of mH compared to *APOE* ε3 homozygotes. This data is consistent with the finding that *APOE* ε4 carriers are at an increased risk for CAA and mH[3, 11, 12]. However, after accounting for differences in Aβ load, the apparent ε4 effect was reduced, suggesting that the risk of mH for *APOE* ε4 carriers is mediated by Aβ load. Similar to *APOE* ε4 carriers, *A* ε2 carriers had a trend of higher numbers of mH*POE* compared to *APOE* ε3 homozygotes Although this was not statistically significant, the apparent effect was not attenuated after accounting for Aβ load, suggesting *APOE* ε2 and Aβ load are largely independent risk factors. Although *APOE* ε2 carriers in the population on average have lower Aβ levels compared to *APOE* ε4 carriers[29], the risk for mH is similar across the two allelic variants in autopsy confirmed CAA patients[30]. The trend of high numbers of mH in APOE ε2 carriers is thought to be associated with vascular fibrinoid necrosis in CAA patients[31, 32], increasing susceptibility to mH in *APOE* ε2 carriers with vascular Aβ. However we note that the subject shown in Figure 2 with the highest number of mH and low ^{18}F-florbetapir uptake was an *APOE* ε2 carrier, which may increase the risk for mH regardless of the low ^{18}F-florbetapir uptake.

We observed an ordered trend of increase in prevalence and numbers of mH from CN to EMCI to LMCI to AD. However, the differences between clinical groups did not reach statistical significance. A similar non-significant trend of higher prevalence of mH was observed in AD compared to CN subjects in other cohorts[4, 13]. Higher numbers of mH were reported in patients with MCI compared to CN[9] and mH was associated with cognitive function in non-demented older adults[33]. In both of the latter studies, subjects were on average over a decade younger than the ADNI cohort, suggesting that age may be an important determinant of the association between mH and cognitive function in older adults.

In a preliminary analysis of the longitudinal data, we found that higher number of mH at baseline are associated with a greater increase in mH at follow-up, a finding in agreement with previous reports on the incidence of mH in memory clinic cohorts[6] and in older adults with no dementia[34]. Incidence rates of mH in the ADNI cohort will be reported in the future

with the availability of longitudinal data in the entire cohort. Furthermore, with serial scanning of subjects, mH identified at baseline will be confirmed on multiple scans, thereby a proportion of the "possible mH" may be diagnosed as "definite mH" with the availability of new scans in individual subjects.

ADNI is an ongoing multi-site prospective study designed to represent cohorts typically recruited to clinical trials for the treatment and prevention of AD. We report that mH is a relatively common imaging finding in the ADNI cohort and the risk of subsequent mH increases with the number of mH at baseline. The prevalence and the risk factors for focal hemosiderin deposits in the ADNI cohort are important considerations for planning treatment and prevention trials with amyloid–modifying agents in AD.

Supplementary Material

Refer to Web version on PubMed Central for supplementary material.

Acknowledgments

Data collection and sharing for this project was funded by the Alzheimer's Disease Neuroimaging Initiative (ADNI) National Institutes of Health Grant U01 AG024904 to MWW. Investigator efforts and data analysis for this study is funded by R01 AG40042 to KK and R01 AG11378 to CRJ. The authors thank Samantha Wille for her help with manuscript formatting and submission.

References

1. Fazekas F, Kleinert R, Roob G, et al. Histopathologic analysis of foci of signal loss on gradient-echo T2*-weighted MR images in patients with spontaneous intracerebral hemorrhage: evidence of microangiopathy-related microbleeds. AJNR Am J Neuroradiol. 1999 Apr; 20(4):637–42. [PubMed: 10319975]
2. Vernooij MW, Ikram MA, Hofman A, Krestin GP, Breteler MM, van der Lugt A. Superficial siderosis in the general population. Neurology. 2009 Jul 21; 73(3):202–5. [PubMed: 19620607]
3. Vernooij MW, van der Lugt A, Ikram MA, et al. Prevalence and risk factors of cerebral microbleeds: the Rotterdam Scan Study. Neurology. 2008 Apr 1; 70(14):1208–14. [PubMed: 18378884]
4. Pettersen JA, Sathiyamoorthy G, Gao FQ, et al. Microbleed topography, leukoaraiosis, and cognition in probable Alzheimer disease from the Sunnybrook dementia study. Arch Neurol. 2008 Jun; 65(6):790–5. [PubMed: 18541799]
5. Jeerakathil T, Wolf PA, Beiser A, et al. Cerebral microbleeds: prevalence and associations with cardiovascular risk factors in the Framingham Study. Stroke. 2004 Aug; 35(8):1831–5. [PubMed: 15155954]
6. Goos JD, Henneman WJ, Sluimer JD, et al. Incidence of cerebral microbleeds: a longitudinal study in a memory clinic population. Neurology. 2010 Jun 15; 74(24):1954–60. [PubMed: 20548041]
7. Kimberly WT, Gilson A, Rost NS, et al. Silent ischemic infarcts are associated with hemorrhage burden in cerebral amyloid angiopathy. Neurology. 2009 Apr 7; 72(14):1230–5. [PubMed: 19349602]
8. Fiehler J. Cerebral microbleeds: old leaks and new haemorrhages. Int J Stroke. 2006 Aug; 1(3):122–30. [PubMed: 18706032]
9. Haller S, Bartsch A, Nguyen D, et al. Cerebral microhemorrhage and iron deposition in mild cognitive impairment: susceptibility-weighted MR imaging assessment. Radiology. 2010 Dec; 257(3):764–73. [PubMed: 20923870]
10. Nakata-Kudo Y, Mizuno T, Yamada K, et al. Microbleeds in Alzheimer disease are more related to cerebral amyloid angiopathy than cerebrovascular disease. Dement Geriatr Cogn Disord. 2006; 22(1):8–14. [PubMed: 16645275]

11. Greenberg SM, Rebeck GW, Vonsattel JP, Gomez-Isla T, Hyman BT. Apolipoprotein E epsilon 4 and cerebral hemorrhage associated with amyloid angiopathy. Ann Neurol. 1995 Aug; 38(2):254–9. [PubMed: 7654074]
12. McCarron MO, Nicoll JA. Apolipoprotein E genotype and cerebral amyloid angiopathy-related hemorrhage. Ann N Y Acad Sci. 2000 Apr.903:176–9. [PubMed: 10818505]
13. Yates PA, Sirisriro R, Villemagne VL, Farquharson S, Masters CL, Rowe CC. Cerebral microhemorrhage and brain beta-amyloid in aging and Alzheimer disease. Neurology. 2011 Jul 5; 77(1):48–54. [PubMed: 21700585]
14. Sperling RA, Jack CR Jr, Black SE, et al. Amyloid-related imaging abnormalities in amyloid-modifying therapeutic trials: Recommendations from the Alzheimer's Association Research Roundtable Workgroup. Alzheimers Dement. 2011 Jul; 7(4):367–85. [PubMed: 21784348]
15. Smith EE, Greenberg SM. Beta-amyloid, blood vessels, and brain function. Stroke. 2009 Jul; 40(7):2601–6. [PubMed: 19443808]
16. Sperling R, Salloway S, Brooks DJ, et al. Amyloid-related imaging abnormalities in patients with Alzheimer's disease treated with bapineuzumab: a retrospective analysis. Lancet Neurol. 2012 Mar; 11(3):241–9. [PubMed: 22305802]
17. Weiner MW, Veitch DP, Aisen PS, et al. The Alzheimer's Disease Neuroimaging Initiative: a review of papers published since its inception. Alzheimer's & dementia : the journal of the Alzheimer's Association. 2012 Feb; 8(1 Suppl):S1–68.
18. Jack CR Jr, Bernstein MA, Borowski BJ, et al. Update on the magnetic resonance imaging core of the Alzheimer's disease neuroimaging initiative. Alzheimer's & dementia : the journal of the Alzheimer's Association. 2010 May; 6(3):212–20.
19. Landau SM, Mintun MA, Joshi AD, et al. Amyloid deposition, hypometabolism, and longitutdinal cognitive decline. Ann Neurol. In Press.
20. Tzourio-Mazoyer N, Landeau B, Papathanassiou D, et al. Automated anatomical labeling of activations in SPM using a macroscopic anatomical parcellation of the MNI MRI single-subject brain. Neuroimage. 2002 Jan; 15(1):273–89. [PubMed: 11771995]
21. Vemuri P, Gunter JL, Senjem ML, et al. Alzheimer's disease diagnosis in individual subjects using structural MR images: validation studies. Neuroimage. 2008 Feb 1; 39(3):1186–97. [PubMed: 18054253]
22. Kantarci K, Senjem ML, Lowe VJ, et al. Effects of age on the glucose metabolic changes in mild cognitive impairment. AJNR Am J Neuroradiol. 2010 Aug; 31(7):1247–53. [PubMed: 20299441]
23. Jack CR Jr, Lowe VJ, Senjem ML, et al. 11C PiB and structural MRI provide complementary information in imaging of Alzheimer's disease and amnestic mild cognitive impairment. Brain. 2008 Mar; 131(Pt 3):665–80. [PubMed: 18263627]
24. Wolk DA, Zhang Z, Boudhar S, Clark CM, Pontecorvo MJ, Arnold SE. Amyloid imaging in Alzheimer's disease: comparison of florbetapir and Pittsburgh compound-B positron emission tomography. J Neurol Neurosurg Psychiatry. 2012 Sep; 83(9):923–6. [PubMed: 22791901]
25. Clark CM, Schneider JA, Bedell BJ, et al. Use of florbetapir-PET for imaging beta-amyloid pathology. Jama. 2011 Jan 19; 305(3):275–83. [PubMed: 21245183]
26. Johnson KA, Gregas M, Becker JA, et al. Imaging of amyloid burden and distribution in cerebral amyloid angiopathy. Ann Neurol. 2007 Sep; 62(3):229–34. [PubMed: 17683091]
27. Dierksen GA, Skehan ME, Khan MA, et al. Spatial relation between microbleeds and amyloid deposits in amyloid angiopathy. Ann Neurol. 2010 Oct; 68(4):545–8. [PubMed: 20865701]
28. Lee SH, Kim SM, Kim N, Yoon BW, Roh JK. Cortico-subcortical distribution of microbleeds is different between hypertension and cerebral amyloid angiopathy. J Neurol Sci. 2007 Jul 15; 258(1–2):111–4. [PubMed: 17449062]
29. Kantarci K, Lowe V, Przybelski SA, et al. APOE modifies the association between Abeta load and cognition in cognitively normal older adults. Neurology. 2012 Jan 24; 78(4):232–40. [PubMed: 22189452]
30. Nicoll JA, Burnett C, Love S, et al. High frequency of apolipoprotein E epsilon 2 allele in hemorrhage due to cerebral amyloid angiopathy. Ann Neurol. 1997 Jun; 41(6):716–21. [PubMed: 9189032]

31. McCarron MO, Nicoll JA, Stewart J, et al. The apolipoprotein E epsilon2 allele and the pathological features in cerebral amyloid angiopathy-related hemorrhage. J Neuropathol Exp Neurol. 1999 Jul; 58(7):711–8. [PubMed: 10411341]

32. Greenberg SM, Vonsattel JP, Segal AZ, et al. Association of apolipoprotein E epsilon2 and vasculopathy in cerebral amyloid angiopathy. Neurology. 1998 Apr; 50(4):961–5. [PubMed: 9566379]

33. Poels MM, Ikram MA, van der Lugt A, et al. Cerebral microbleeds are associated with worse cognitive function: the Rotterdam Scan Study. Neurology. 2012 Jan 31; 78(5):326–33. [PubMed: 22262748]

34. Poels MM, Ikram MA, van der Lugt A, et al. Incidence of cerebral microbleeds in the general population: the Rotterdam Scan Study. Stroke. 2011 Mar; 42(3):656–61. [PubMed: 21307170]

Research in Context

Systematic review

Review of the literature was performed using PubMed with the following key words: microhemorrhage, microbleed and superficial siderosis. Articles focusing on the prevalence, incidence and risk factors for focal hemosiderin deposits were selected for inclusion in this manuscript.

Interpretation

Focal hemosiderin deposits are relatively common in the ADNI cohort, an important consideration when planning amyloid–modifying trials for treatment and prevention of AD. Although the number of microhemorrhages is associated with β-amyloid load, a robust relationship between localized ^{18}F-florbetapir uptake and microhemorrhage density was not observed.

Future directions

Incidence rates of mH in the ADNI cohort will be reported in the future with the availability of longitudinal data in the entire cohort.

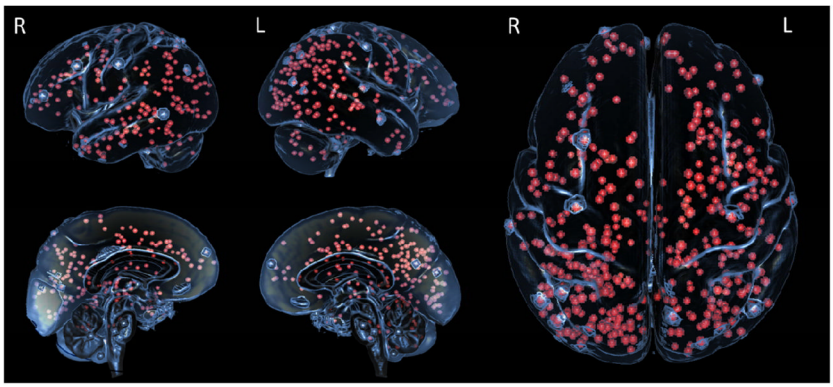

Figure 1. Distribution of Individual Microhemorrhages at Baseline

The rendered image is the union of the composite distance map and a skull stripped version of the custom T1 template. The T1 image is thresholded such that the surface shown is approximately in the middle of the grey matter ribbon in template space. “Pock marks” on the rendered surface are associated with mH spheres right at the selected surface. One outlier with 264 mH at baseline was not included in the composite maps.

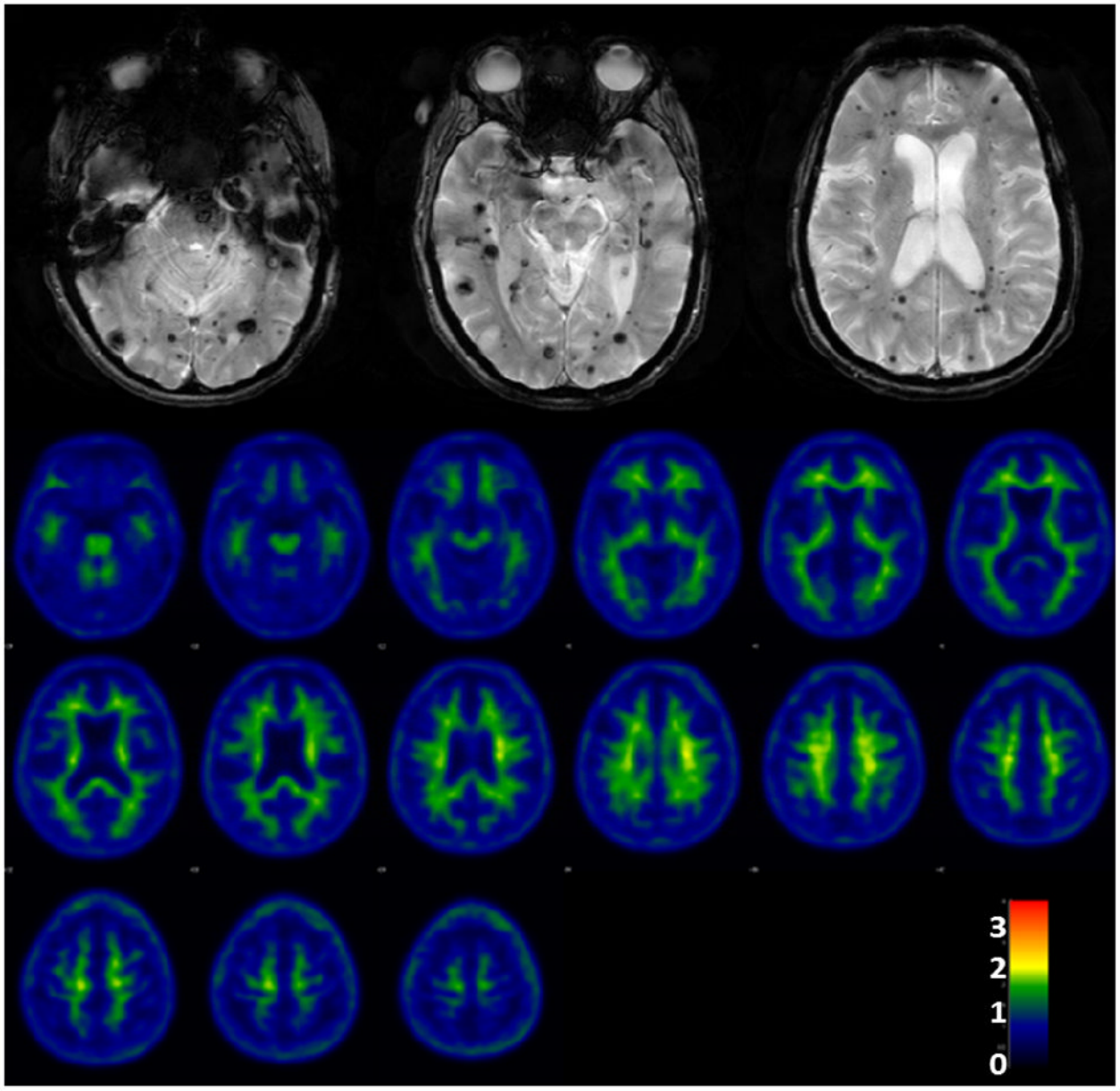

Figure 2. Early Mild Cognitive Impairment Subject with 264 Microhemorrhages and Low Cortical ^{18}F-florbetapir Uptake

T2* GRE (upper panel) and ^{18}F-florbetapir SUVR (lower panel) images are shown with a similar color scale.

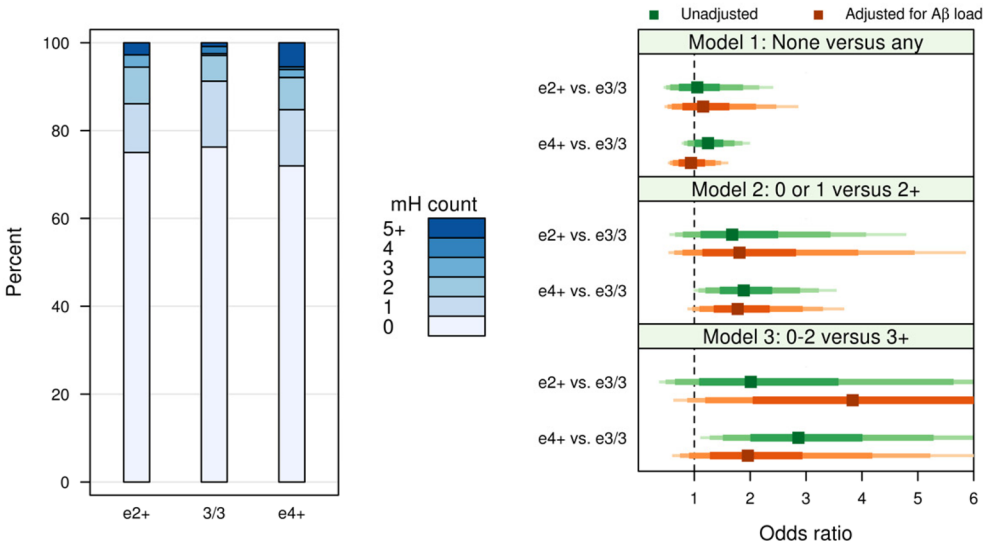

Figure 3. Microhemorrhage Count by *APOE* Genotype

Bar plots of the distribution of mH count by *APOE* genotype (left); Odds ratios and confidence intervals from logistic models for three different definitions of the mH event both adjusted (orange) and unadjusted (green) by β-Amyloid load (right). The confidence intervals use shading to indicate the 95% CI, the 90% CI, the 80% CI, and the 50% CI.

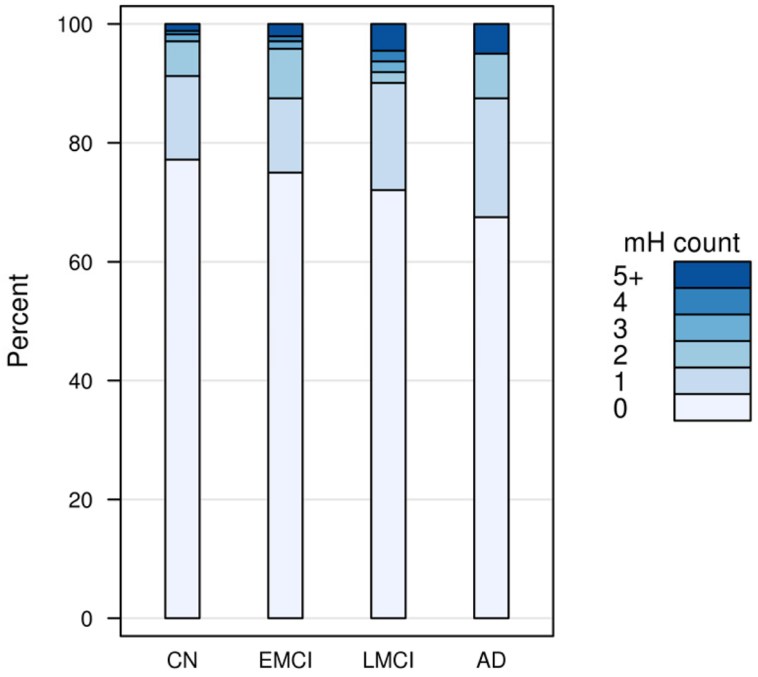

Figure 4. Microhemorrhage Count by Clinical diagnosis
Bar plots of the distribution of mH count by clinical diagnosis.

Table 1

Patient characteristics at baseline MRI

Characteristic	CN	EMCI	LMCI	AD	*P*[*]
Number of subjects	171	240	111	40	—
Female gender, n (%)	89 (52)	109 (45)	51 (46)	18 (45)	0.56
Age at MRI, median (IQR), y	73 (70, 78)	71 (65, 76)	73 (67, 78)	79 (71, 83)	<0.001
Education, median (IQR), y	16 (15, 19)	16 (14, 18)	16 (15, 18)	16 (14, 18)	0.01
APOE genotype, n (%)[**]					0.002
2/2 or 2/3	15 (11)	17 (8)	4 (6)	0	
3/3	89 (65)	107 (53)	32 (45)	12 (41)	
2/4	0	4 (2)	2 (2)	0	
3/4 or 4/4	34 (25)	78 (39)	35 (49)	17 (59)	
MMSE score, median (IQR)	29 (28, 30)	29 (28, 30)	28 (26, 29)	23 (22, 25)	<0.001
CDR global score, n (%)					<0.001
0	168 (99)	0	2 (2)	0	
0.5	2 (1)	240 (100)	108 (97)	12 (30)	
1	0	0	1 (1)	27 (68)	
>1	0	0	0	1 (2)	
CDR Sum of Boxes score, median (IQR)	0 (0, 0)	1 (0, 2)	2 (1, 2)	5 (4, 6)	<0.001

Abbreviations: AD, Alzheimer dementia; *APOE*, appolippoprotein E; CDR, Clinical Dementia Rating; EMCI, Early mild cognitive impairment; IQR, inter-quartile range LMCI, Late mild cognitive impairment; MMSE, Mini Mental State Exam;

[*] Gender and *APOE* genotype differences among clinical groups were tested with a chi-squared test. Other variables tested with a non-parametric Kruskal-Wallis test.

[**] As of July 1, 2012, 116 subjects missing *APOE* genotype.

Table 2

Regional mH density, regional ^{18}F-florbetapir SUVR and their association

Region	Mean (SD) mH density (count/L)***	Mean (SD) ^{18}F-AV-45 SUVR	Spearman correlation *
Frontal	0.70 (7.7)	1.62 (0.28)	0.12(0.002)
Temporal	0.96 (8.9)	1.43 (0.25)	0.03 (0.14)
Parietal	0.1 (10)	1.63 (0.30)	0.1 (0.01)
Occipital	1.3 (14)	1.49 (0.23)	0.06 (0.06)
Deep/infratentorial **	0.59 (6.1)	1.13 (0.05)	−0.02 (0.57)

* Rank correlation shown is between mH density and ^{18}F-florbetapir SUVR for the indicated region

** Includes subcortical GM and WM plus brainstem

*** mH density is defined by the number of definite mH in each region divided by the volume of the region